Conference Paper/Konferans Bildirisi

GAZİ
JOURNAL OF ENGINEERING SCIENCES

CLAHE based Enhancement to Transfer Learning in COVID-19 Detection

Gokhan Altan*[a], Süleyman Serhan Narlı [b]

Submitted: 02.12.2021 Revised: 11.04.2022 Accepted: 29.04.2022 doi:10.30855/gmbd.0705001

ABSTRACT

Early diagnosis of COVID-19 disease becomes possible with the enhancements on feature learning and advanced pre-processing stages for classification of chest X-ray images using deep learning. Besides, high-performance models have been developed by many researchers due to the popularity of Deep Learning. In this study, chest X-ray images were pre-processed using Contrast Limited Adaptive Histogram Equalization (CLAHE) before the classification with particular popular transfer learning approaches in deep learning architectures including AlexNet, MobileNet, VGG16, and DarkNet19. The originality of the paper is pre-processing the images using CLAHE to obtain more significant representations of airways and pathologies instead of training with raw chest X-ray images. The best CLAHE parameters were determined considering the results of various trials at a specified range. The other superior contribution of the proposal is using a large-scale dataset, which is comprised of 3500 healthy and 3615 chest x-rays with COVID-19. The CLAHE-based transfer learning proposal achieved an accuracy rate of 95.878% as the most successful binary classification result for COVID-19 and healthy using VGG16 model and CLAHE parameters including disk value of 56, clip-limit of 0.2.

Keywords: Deep Learning, Convolutional neural networks, Adaptive Histogram Equalization, medical image analysis, chest x-ray

[a,*] Iskenderun Technical University, Faculty of Natural and Engineering Sciences, Dept. of Computer Engineering 31200 - Hatay, Türkiye
Orcid: 0000-0001-7883-3131
e mail: gokhan.altan@iste.edu.tr

[b] Iskenderun Technical University, Faculty of Natural and Engineering Sciences, Dept. of Computer Engineering 31200 - Hatay, Türkiye
Orcid: 0000-0003-0162-9786
e mail: serhan.narli@gmail.com

*Corresponding author: gokhan.altan@iste.edu.tr

COVID-19 Tespitinde Öğrenim Aktarımına CLAHE Tabanlı Geliştirme

ÖZ

Derin öğrenme kullanılarak göğüs röntgeni görüntülerinin sınıflandırılması için öznitelik öğrenme ve gelişmiş ön işleme aşamaları üzerindeki geliştirmelerle COVID-19 hastalığının erken teşhisi mümkün hale getirmiştir. Bunun yanında, Derin Öğrenme popülaritesi nedeniyle birçok araştırmacı tarafından denenerek yüksek performanslı modeller ortaya sürülmüştür. Bu çalışmada göğüs röntgen filmlerine, AlexNet, MobileNet, VGG16 ve DarkNet19 gibi popüler derin öğrenme mimarilerindeki transfer öğrenme yaklaşımıyla sınıflandırmadan önce Kontrast Sınırlı Adaptif Histogram Eşitleme (CLAHE) kullanılarak ön işlem uygulanmıştır. Makalenin orijinalliği, göğüs röntgeni görüntülerini doğrudan ham veri ile eğitmek yerine önce hava yollarının ve patolojilerin daha belirgin yansımalarını elde edilerek gerçekleştirilmesidir. En başarılı CLAHE parametreleri çeşitli aralıklardaki deneyler sonucunda belirlenmiştir. Önerilen yaklaşımın diğer üstün katkısı, modelin eğitiminde ve testinde 3615 COVID-19'lu ve 3500 sağlıklı göğüs röntgeninden oluşan büyük ölçekli bir veri seti kullanılmasıdır. CLAHE tabanlı öğrenim aktarımı önerisi, en başarılı COVID-19 ve sağlıklı ikili sınıflandırma başarımına %95,878 doğruluk oranıyla VGG16 modeli üzerinde 56 disk değeri ve 0.2 klip limiti CLAHE parametrelerini kullanarak ulaşmıştır.

Anahtar Kelimeler: Derin Öğrenme, Evrişimsel sinir ağları, Göğüs röntgeni, Adaptif Histogram Eşitleme, Tıbbi görüntü analizi

To cite this article: G. Altan and S.S. Narlı, "CLAHE based Enhancement to Transfer Learning in COVID-19 Detection," *Gazi Journal of Engineering Sciences,* vol. 8, no. 2, pp. 406-416, 2022. doi:10.30855/gmbd.0705001

1. Introduction

Severe acute respiratory syndrome coronavirus (COVID-19), a new type of coronavirus of which the first known presence was reported in December 2019. It has affected the whole world and caused thousands of death across the globe. Early diagnosis is essential to reduce the effects of the COVID-19 virus. Many methods are used to detect the COVID-19 virus, and one of the fastest methods is detecting COVID-19 disease by chest X-ray (CXR), the diagnosis used. In terms of the cost of the methods, X-ray images are accepted as a high-speed and cheap method compared to other diagnostic procedures. Preventing the progression of the disease on the lungs in COVID-19 disease by early diagnosis is of vital importance, which increases the volume of computerized analysis on X-rays.

X-ray is an inexpensive radiology test that creates an image of the chest and internal organs with low-dose radiation without uncomfortable for the patient. The chest is quickly exposed to radiation by a specialized medical device to perform a chest X-ray. Consequently, an image is generated on a film by the permeability specifications of the tissues [1].

Diagnosing by CXR images is considered a difficult task for even radiologists in terms of small pathologies and early stages of common lung diseases. Therefore, computer-aided diagnosis (CAD) systems have been developed in recent years to assist physicians in evaluating a CXR image. However, the enhancing CAD systems have not yet achieved satisfactory results in the diagnosis and prognosis of diseases on CXR images [2].

Due to the necessity for rapid and accurate analysis of CXR images, a series of COVID-19 detection models based on state-of-the-art Convolutional neural network (CNN) models have been proposed in recent years, with promising results [3]. Apostolopoulos (2020) experimented with two different datasets using learning transfer for CXR image analysis. The first dataset contains 224 COVID-19 images, 700 Bacterial Pneumonia, and 504 Healthy images. In the first analysis, he experimented with five different CNN models. The highest binary classification results were obtained with VGG19 with 98.75% among the VGG19, MobileNet v2, Inception, Xception, and Inception ResNet v2 models. Consequently, the most successful model achieved a classification accuracy rate of 93.48%, a precision rate of 92.85%, and a sensitivity rate of 98.75% for multiclass classification (healthy, COVID-19, and pneumonia). The other dataset consists of 224 COVID-19, 714 pneumonias (400 bacterial and 314 viral pneumonia), and 504 healthy CXRs. The second experiment achieved a classification performance of 96% using transfer learning on MobileNet v2 for binary cases. Moreover, they reached the performance rates of 94.72%, 98.66%, and 96.46% for accuracy, precision, and sensitivity for multiclass cases, respectively. Apostolopoulos evaluated the capabilities of transfer learning for various classification performances of different CNN architectures on CXR images. They highlighted the most success of VGG19 and MobileNet v2 for the diagnosis of COVID-19 [4]. Chowdhury (2020) trained CXR images using MobileNetV2, ResNet18, ResNet101, VGG19, and DenseNet201 models. Before training the CNN architectures, they performed preprocessing and segmentation for the CXR dataset. In the preprocessing step, the data set is reduced to 224,224 for the models we mentioned above. The dataset has been resized to two dimensions with 227x227 pixels for SqueezeNet and 299x299 for the Inception v3 model. In the segmentation process, the images are rotated and flipped. The training of CNN architectures was conducted without applying segmentation processes to the images. They utilized 423 COVID-19, 423 viral pneumonias, and 423 healthy CXR images in the experiments (304 for training, 85 for testing). They segmented 2128, 2274, and 1579 regions of interest for pathologies and healthy tissues. In both experiments, 5-fold cross-validation was performed in the training of the CNN models. The ChexNet architecture reached the best classification performance without segmentation for 2-class training with an accuracy rate of 99.41%, the precision rate of 99.42%, the sensitivity rate of 99.41%, and the f1-score of 0.9941. After applying the segmentation process, the success rate was 99.69%, precision 99.69%, sensitivity 99.69%, and f1-score 99.69%. The ChexNet without segmentation achieved an accuracy rate of 97.74%, precision rate of 96.61%, sensitivity rate of 96.61%, and f1-score of 0.9661 for the multiclass case analysis. The best diagnosis achievements for segmented CXR images were reported an accuracy rate of 97.94%, precision rate of 97.95%, sensitivity rate of 97.94%, and f1-score of 0.9794 using DenseNet201 architecture. They examined the effect of the segmentation on the performance for 2-class and multiclass diagnoses. Moreover, they determined well enough classification performances on various CNN models [3].

Medical images are diagnostic tools for imaging, visualization, and identification of pathological nodules and tissues from healthy tissue. Many medical imaging modalities visualize the density of organs based on a given dose of x-ray or photon exposure. CXR, which is used to detect lung and heart diseases, is often preferred because it contains low-dose radiography that is not harmful to human health and is cheaper than computed tomography. It is still used as the first choice in the physical experiments of clinical validity for a supportive diagnosis, an indispensable tool for visceral ailments such as lungs, heart, bone, kidney, and intestines [5]. Severe lung diseases can be detected in lung tomography due to the intense appearance of pathological cells in the tissue. For this reason, chest radiographs still come to the fore as the primary approach for imaging respiratory tract diseases and early detection of most pathologies. Due to the noisy chest x-rays, detecting disease pathology requires an extensive workload for specialists and additional time loss for double-blind evaluation of each case. Such disadvantages can be overcome in a short time using CAD systems by detecting minor pathologies that may be overlooked even by multiple radiologists and speed up the patient-specific treatment process [6].

Dataset and feature extraction are very important in machine learning algorithms to develop successful CAD models with clinical validity. Arranging the distribution of training and test data in the dataset are operations to consider when modelling a robust and trusting CAD system [7].

Traditional CAD models in CXR analysis must be trained by including the characteristics of pathological regions. Moreover, it is essential to generate the small pathology, edema, and nodules in the airways to detect pathological regions depending on high classification performances with related activation maps. Especially in lung diseases, airways, obstructions, damages, and edema regions need to be improved with sensitive image processing approaches for diagnosis and visualization at early stages with a clinical usability [5]. Due to CXR being a noisy medical image, certain pre-processing has become necessary. However, filtering techniques and pre-processing of the overall CXRs cause a distortion of the pathologies representing the disease symptoms and losing the regional importance of pathologies. Significantly, clarification of disease-specific pathologies and enhancing airways before feeding the classifier will increase the clinical validity of the learning procedure for deep learning type classifiers. Therefore, the determination of CLAHE parameters that should be used for different popular pre-trained architectures for abnormalities in COVID-19 is a major deficiency in the literature.

This study aimed at making pathological regions more prominent in CXR using Adaptive Histogram Equalization (AHE). The CXR images were trained with lightweight popular deep learning models for various ranges of AHE parameters. In this way, the best AHE parameters were determined according to the highest achievements in test and training for each CNN architecture.

We proposed a simplistic CNN-based COVID-19 identification model for separating COVID-19 cases from healthy subjects. The main contribution is feeding the CNN architectures with apparent pathology with a clinical validity for simplistic transfer learning procedures on a large-scale dataset.

2. Material and Method

2.1. Convolutional Neural Networks

Convolutional Neural Network (CNN) is a multi-layered feed-forward neural network, which is located within the layers of deep learning. It is comprised of filtering stages using convolution and generating feature activation maps. The CNN produces prominent representations by feature learning. The dominant pixel values of the feature maps can be increased using various sizes and maps of filters. Therefore, it is not necessary to use any additional feature extraction or hand-crafting feature algorithms for the input data [8].

CNN architecture was first presented by LeCun et al. with the name of LeNet. They revealed this procedure on a gradient basis which is comprised of feature learning with convolution and classification stage for feeding the supervised learning-based approach [9].

CNN is a deep network model consisting of convolutional layers, transferring the dominant pixels using pooling layers. Each stage of architecture generates a various number of feature maps. Each pixel value in a feature map has a receptive field that connects to a layer of neurons in the previous layer via a trainable weight set in the flattening layer [10]. The inputs are combined with the learned weights to create a new feature map, and the results are sent via rectified linear units (ReLUs; [11]), a non-linear activation function.

The weights of all neurons in a feature map are equally constrained. However, different feature maps in the same convolution layer have different weights. Therefore, various features can be extracted at each location and transferred between convolution blocks. The convolution layer uses various sizes and numbers of filters to represent different characteristics of the input images. The depth of the CNN is defined by the number of filters in each convolution layer [12].

Deep learning models also include the pooling layer, which reduces the input data size separately from the convolution layer. It is generally used after the activation layer at the end of convolutional blocks. The jointing process creates data losses. However, it makes the network faster with the decrease in the dimensionality of represented images to be circulated in the neural networks. Thus, the amount of computation in the CNN and the memory size for the analysis are reduced [13]. After several convolution layers and pooling layers, the feature maps are stacked on top of each other, and they flattened to the fully-connected layers to interpret the representations and to perform a supervised classification [14].

The fully-connected layer produces the classification result according to the desired number of classes depending on a particular function. The softmax activation function is generally used at the output function of the classification layer to predict proportional similarity of the actual output [12].

2.2. COVIDx Dataset

Chest X-rays with COVID-19 were obtained from the COVIDx dataset [15], the largest open-access dataset in terms of the number of COVID-19 positive cases. It consists of 3616 chest X-rays that are positive for COVID-19 and continue to be updated due to ongoing cases worldwide. It has been analysed as part of the Italian Medical Association, Interventional Radiology (SIRM) COVID-19 database and the COVID-19 dataset.

The CXRs have a wide variation in specifications in terms of resolution and depth. Therefore, each CXR image needs to be resized in a standard form. However, pneumonia and healthy CXRs are rectangular (Ex: 1900x140), COVID-19 cases are square (299x299). In this way, the rectangular chest x-ray is resized to square form and stretched, causing loss of the anatomical shape of the lungs. For this reason, square resizing of chest X-rays and zero translation were applied to prevent distortion while preserving the anatomical shape of the lungs.

The CXRs were selected from the COVIDx database. A total number of 7115 CXRs (3615 COVID-19 and 3500 healthy) were analysed to evaluate the effect of the transfer learning on enhanced CXRs for classification of COVID-19 and healthy cases.

2.3. Transfer Learning

Successful training of deep neural networks usually requires a large-scale dataset and a long training time. Moreover, a fundamental assumption for many deep learning models is that training and testing data should be taken from a similar distribution. When the number of data is less than necessary to train the model, it is essential to reuse previous knowledge for different data, tasks, or feature sets. Transfer learning is a novel deep learning approach in which a previously trained model is reused as the starting point for a related model and task. It not only reduces the necessity to collect a large number of training data but also speeds up the training of deep learning architectures [16,17].

Traditionally, Deep neural networks require huge amounts of labelled datasets for image classification, such as ImageNet [18], one of the largest datasets (more than 14 million images from 1000 objects)

very powerful. However, transfer learning has recently been an effective solution in medical image recognition systems with a shortage of labelled datasets. Training of deep learning from scratch can be computationally expensive. In this context, two transfer learning techniques have been widely applied for image recognition tasks: (1) using pre-trained architectures as a feature extractor and (2) fine-tuning a pre-trained network with adaptive parameter updates [5].

This study utilized transfer learning on the popular lightweight CNN architectures, including AlexNet, VGG16, DarkNet19, and MobileNet.

AlexNet is one of the pioneer studies to popularize convolutional neural networks in deep learning. AlexNet [19] significantly outperformed other handcrafted models in the 2012 ImageNet ILSVRC competition. It is composed of five convolutional layers, three max-pooling, and three fully connected layers.

The VGGNet performed very successfully in the ILSVRC competition in 2014 [20]. 6 different convolution layer models are proposed for the various designed architecture (11, 13, 16, and 19 convolution layers accordingly). In this architecture, the convolution filter size was chosen as 3x3 [21].

MobileNet architecture has been introduced with a deeply separable convolution layer instead of the traditional convolution layer [22]. It has a two-dimensional spatial separable convolution by dividing the two-dimensional (height-width) filter into two small kernels. It requires far fewer learned parameters than a regular convolution layer with the same procedure.

The DarkNet19 architecture has been proposed as a novel classification model which is based on the YOLOv2 model [23]. Similar to the VGG model, a 3x3 convolution filter is used, and the number of filters is doubled after each maximum value association layer. In the classification layer, the feature representation is revealed by using a 1x1 dimensional convolution filter between the mean pooling and the 3x3 dimensional convolution layer [24]. DarkNet19 architecture is comprised of 19 convolution layers, five max-pooling layers.

2.4. Contrast Limited Adaptive Histogram Equalization

Contrast Limited Adaptive Histogram Equalization (CLAHE) is a technique used to enhance the density level of an image. CLAHE is frequently used in medical image processing for pixel density level rearrangement and noise removal [25]. CLAHE was developed as variations of histogram equalization by Hummel [26,27], Ketcham [28], and Pizer [29]. It has performed successful enhancing results on various types of images. Unlike general histogram equalization, CLAHE operates based on a defined intensity level on regional pixels of the image rather than handling the intensity level of the total image. To eliminate the noise in the image, the increase in intensity level is limited [30]. Unlike adaptive histogram equalization (AHE), CLAHE updates the density value according to a user-specified maximum (clip-limit) value. Thus, the density level does not affect the smooth regions and prevents the excessive increase as a noise. As a result, CLAHE determines the pixel radius to which the histogram equalization will be applied as in AHE, but also it has a user-defined density limit (clip-limit), unlike AHE. Thus, the details in the image become more prominent [29].

Figure 1 indicates the enhancement outputs and pixel contrast distributions on a random CXR for various histogram equalization techniques. The original CXR exhibits an unstable distribution with pixel contrast values stacked between 0.25 and 0.75. Although this pixel contrast value is distributed in the range of 0-1 after conventional Histogram equalization (HE), its consistency is not at a sufficient level. Although a more consistent distribution is obtained for values in the pixel contrast range by using Local histogram equalization (LHE), the contrast values of 0 and 1 have a high value in the distribution. Therefore, the rib cages bones and airway sections on the CXR become similar visibility in the enhanced image. When using the same disk size as LHE for CLAHE, 0 and 1-pixel contrast values are reduced to almost zero even for a low clip-limit of 0.02. Compared to LHE, CLAHE provided clearer visibility in contrast with a regional enhancement for bone tissue with poor permeability of the airways.

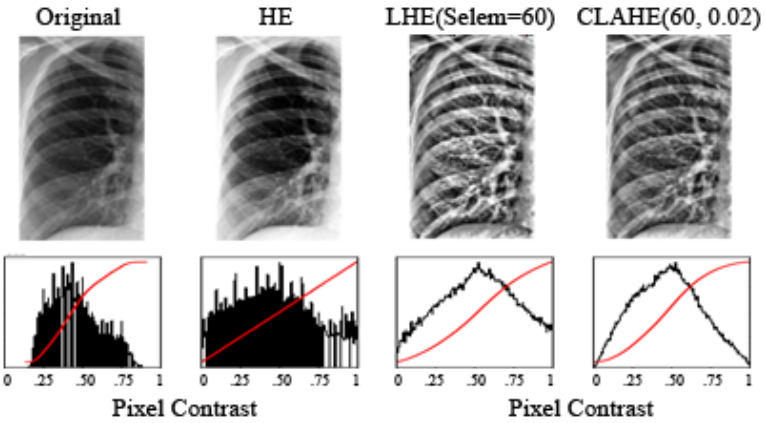

Figure 1. Different Histogram Equalization Methods

The pioneering studies that reported successful enhancements on chest X-ray films utilized disc sizes of 1/8 - 1/16 of the input and clip limit values of 0.2 and 0.3 [25], [31]. In this study, we additionally analysed the effect of the disk sizes of [1/2, 1/4, 1/7, 1/8, 1/16, 1/28, and 1/56] with input size of 224 and clip limit values at the range of [0-1] increasing by 0.1 to increase the scope of experiments. By determining the variations, it was desired to determine the most responsible CLAHE parameters for learning the pathologies with COVID-19. We experimented a brute force on the parameters of CLAHE, including clip-limit and disc size. According to the best performances on separating COVID-19 from healthy subjects, the five highest-performing CLAHE parameters were presented for each deep learning architecture.

Figure 2. A random CXR with COVID-19 (left) and its output with the best CLAHE parameters for DarkNet19, AlexNet, VGG16, and MobileNet, respectively

3. Experimental Results and Discussion

Transfer learning focuses on the architectures which update the pre-trained weights on large-scale datasets. There are many object-oriented programming languages that support transfer learning on interfaces and procedures. Python is the most common language with easy integration, GPU-based computational capabilities. Hence, we utilized Python language with Tensorflow and Keras libraries for training the CNN models. In this process, Anaconda's Spyder interface was preferred. Each training was conducted using Intel Core i7-10750H CPU (2.60 GHZ) and Nvidia RTX 2060 Graphics card in terms of hardware.

3500 Healthy CXR images and 3615 COVID-19 CXR images were trained for different CLAHE parameters with AlexNet, MobileNet, VGG16, and DarkNet19 models.

We experimented 71 combinations for various disk size and clip-limit values of CLAHE parameters. The most successful five disk size and clip-limit values were stored for each deep learning model among the entire achievements. Figure 3 indicates the determination procedure for CLAHE on transfer learning with different pre-trained architectures. COVID-19 and healthy CXR images were preprocessed using the best five CLAHE parameters, and the dataset was rearranged according to different contrast values. In the training of the diagnosis model, the dataset is divided into 80% training and 20% testing folds, the batch size value is 32, and the epoch number is 50. An early stopping algorithm was triggered to prevent overfitting during the learning of the deep learning architecture. The CLAHE parameters evaluated for each pre-trained architecture and the best five achievements are presented in Table 1. Figure 2 depicts the enhanced CXRs with the best CLAHE parameters for DarkNet19, AlexNet, VGG16, and MobileNet.

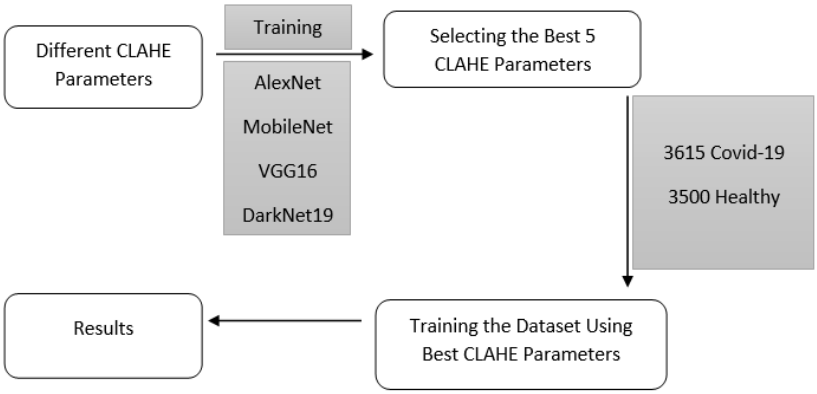

Figure 3. CLAHE Parameters selection procedure

Table 1. Comparison of classification performances for CLAHE parameters on each CNN model

	Disk Value	Clip Limit Value	Accuracy	Precision	Recall	F1-Score
	8	0.1	0.89227	0.90162	0.89227	0.89155
	4	0.4	0.90070	0.91511	0.90070	0.89993
DarkNet19	8	0.6	0.92319	0.92849	0.92319	0.92299
	16	0.7	0.94239	0.94283	0.94239	0.94238
	112	1	0.95176	0.95447	0.95176	0.95166
	4	0.1	0.91216	0.91581	0.91216	0.91194
	8	0.1	0.84118	0.87389	0.84118	0.83777
AlexNet	56	0.1	0.85151	0.87877	0.85152	0.84903
	28	0.5	0.93724	0.93770	0.93724	0.93723
	56	0.8	0.83794	0.87431	0.83794	0.83360
	28	0.4	0.82763	0.82872	0.82763	0.82743
	28	0.6	0.80468	0.80570	0.80468	0.80444
MobileNet	32	0.7	0.81827	0.82020	0.81827	0.81790
	28	0.5	0.81358	0.81701	0.81358	0.81320
	8	0.9	0.77986	0.78647	0.77986	0.77835
	4	0.1	0.95550	0.95619	0.95550	0.95550
	28	0.1	0.95410	0.95460	0.95410	0.95408
VGG16	8	0.2	0.89602	0.90940	0.89602	0.89506
	56	0.2	0.95878	0.95955	0.95878	0.95876
	8	0.3	0.88852	0.90031	0.88852	0.88780

Early diagnosis of diseases with CAD systems has gained significant importance by analyses in terms of COVID-19. Consequently, developing novel image processing techniques, definition of model-based enhancement parameters, and proposing robust systems have become researchers' main focuses.

The studies for assessments of COVID-19 and using automatized techniques for abnormality detection within various diagnostic tools became very important to early diagnosis. Whereas high classification performances for diagnosis of COVID-19 were reported using different deep learning models with complicated architectures, applying simple pre-processing stages to the evaluation process reached high enough achievements using pruned and simplistic architectures on transfer learning.

The main ideas are using the generated representations instead of many convolutional layers, transmitting feature learning within resembled instances with CLAHE, and adapting the capability of feature transferring between adjacent layers to separate healthy CXRs from COVID-19 pathology.

The state-of-the-art indicates that the pre-trained CNN architectures, pruned networks, and detailed feature learning stages have the ability to separate COVID-19 from healthy cases on CXRs. Using hybrid methods resembling the stage of deep architectures, pruning the complex pre-trained architectures with transfer learning, and proposing lightweight architectures with simplistic image processing approaches can advance the deep models. The experimented pruned pre-trained CNN architecture with CLAHE is a powerful trajectory to get high enough classification performances with easy-adaptable real-time applications over to the state-of-art. Using CLAHE for generating smoothed representation provided high classification performances using transfer learning on popular CNN architectures. Therefore, simplifying the deep architectures reduces the training time of the COVID-19

identification architectures and integrates the shallow architectures for even real-time applications in embedded systems.

Table 2. Comparison of relevant DL-based COVID-19 disease detection studies in terms of algorithms and performances

Related Works	Preprocessing	Model	Covid-19 Sample	Healthy Sample	Accuracy (%)
Narin et al. [32]	-	ResNet50	50	50	98.00
Castiglioni et al. [33]	-	ResNet10	250	250	80.00
Haghanifar [34]	HE, CLAHE, Segmentation (U-NET)	DenseNet121	400	3000	98.68
Das et al. [35]	-	InceptionNet v3	50	50	97.00
Saha et al. [36]	-	EMCNet (VGG16)	2300	2300	98.91
This study	CLAHE (Disk:112, Clip_limit:1)	DarkNet19	3615	3500	95.176
	CLAHE (Disk:28, Clip_limit:0.5)	AlexNet	3615	3500	93.724
	CLAHE (Disk:28, Clip_limit:0.4)	MobileNet	3615	3500	82.763
	CLAHE (Disk:56, Clip_limit:0.2)	VGG16	3615	3500	95.878

Table 2 presents the comparison of our study with the deep learning algorithms developed for COVID-19 binary classification diagnosis. Narin et al. used 50 healthy and 50 COVID-19 CXRs for training and testing of ResNet50 [9]. They applied cross validation method with in the training of pre-trained model and achieved an accuracy rate of 98% [32]. Castiglioni et al. presented a completely different approach on own dataset, including 250 COVID-19 cases and 250 healthy images. The ResNet10 model [9] was trained with an accuracy rate of 80% on their limited CXR dataset [33]. Haghanifar et al. analysed a total number of 10380 images from 780 COVID-19, 5000 healthy, and 4600 NIH CXR-14 dataset. The contrast of the images was adjusted using histogram equalization thereby making the mass and nodules more prominent using CLAHE algorithm. The semantic segmentation was applied with U-Net on enhanced CXRs, so that the lung lobes were detected from the image and segmented. They proposed own architecture, the COVID-CXNet model which is built from the CheXNet-based model and is composed of 431 layers about 7M parameters. The advantage of the architecture is reducing trains time by high speed. On the other hand, it was created from 5 convolution layers and fully connected layers on a limited number of CXRs with COVID-19 and reported an accuracy rate of 96.72%. The best achievements for healthy and 400 COVID-19 CXRs were 98.68% and 94.00% for accuracy and f1-score, respectively. Their proposal emphasized too complicated with segmentation procedure, CLAHE on segmented lung lobes, and hybrid deep learning architecture [34]. Das et al. proposed a modified version of the InceptionNet v3 model in their study. Due to the lack number of COVID-19 CXRs, InceptionNet v3 model on ImageNet weights was re-trained by aiming to prevent overfitting with its architectural complicated architecture. Consequently, they reached classification performances on limited testing CXRs (50 COVID-19 and 50 healthy) with rates of 97.00%, 94.00%, and 100% for accuracy, sensitivity, and specificity on InceptionNet v3, respectively [35]. Saha et al. utilized CNN as feature learning and conventional machine learning classifiers (random forest, support vector machine, decision tree, and AdaBoost) to classify COVID-19 cases. A total number of 2300 (from different sources) CXRs with COVID-19 and 2300 healthy CXRs were analysed in the training of CNN. Their proposal, EMCNet, was inspired by the VGG-16 architecture with the advantages of transfer learning. The highest classification performances for binary classification were an accuracy rate of 98.91%, precision rate of 100%, recall rate of 97.82% and f1-score 0.9889. In their analysis, the accuracy rate was maximized by using conventional machine learning classifiers by stated a different way in classification on the advanced joint use of features extraction by deep learning [36].

The common point and main disadvantage of all studies is that they used a low number of CXRs with COVID-19. Moreover, using raw CXRs has no ability to assess abnormality in common lung diseases. Therefore, it is not possible to define a standardized in the clinical validity. The proposal analysed a large number of CXRs with COVID-19, homogenous distribution of binary cases, and enhanced abnormalities related to the COVID-19. The proposal reached the highest classification accuracy with rate of 95.878 using VGG16 architecture.

3. Conclusions

Processing medical images with Deep Learning has become very popular in recent years. Its use is increasing daily due to its high performance and easy adaptability for classification in various fields, even medical image processing. Deep Learning includes many parameters originated from the inspired by an advanced neural network structure. Resultant to its high performance in the classification of medical images, it is used to classify many diseases. Although many measures force the worldwide effects of COVID-19 (SARS-CoV-2) disease as a pandemic, the variants of COVID-19 disease have not been prevented. Under these circumstances, the necessity and the success of early diagnosis of COVID-19 progression are in direct proportion for treatments. In this case, the importance of early detection systems emerges.

The main contribution of the paper is adapting simplistic CNN architectures with the enhanced medical images applying CLAHE for classification of healthy CXRs and CXRs with COVID-19. Moreover, utilizing updated large-scale COVID-19 CXRs (3615 cases) proves the clinical availability of the proposal on defined parameters with CNN.

Conflict of Interest Statement

No potential conflict of interest was reported by the authors.

References

[1] S. Jaeger *et al.*, "Automatic Tuberculosis Screening Using Chest Radiographs," *IEEE Transactions on Medical Imaging*, vol. 33, no. 2, pp. 233–245, 2014. doi:10.1109/TMI.2013.2284099

[2] A. A. El-solh, C. Hsiao, S. Goodnough, J. Serghani, and B. J. B. Grant, "Predicting active pulmonary Tuberculosis Using an Artificial Neural Network," *Chest*, vol. 116, no. 4, pp. 968–973, 1999. doi:10.1378/chest.116.4.968

[3] M. E. H. Chowdhury *et al.*, "Can AI Help in Screening Viral and COVID-19 Pneumonia?," *IEEE Access*, vol. 8, pp. 132665–132676, 2020. doi:10.1109/ACCESS.2020.3010287

[4] I. D. Apostolopoulos and T. A. Mpesiana, "Covid-19: automatic detection from X-ray images utilizing transfer learning with convolutional neural networks," *Physical and Engineering Sciences in Medicine.*, vol. 43, no. 2, pp. 635–640, 2020. doi:10.1007/s13246-020-00865-4.

[5] G. Litjens *et al.*, "A survey on deep learning in medical image analysis," *Medical Image Analysis*. vol.42, pp. 60–88, 2017, doi: 10.1016/j.media.2017.07.005

[6] S. Rajaraman, S. Sornapudi, M. Kohli, and S. Antani, "Assessment of an ensemble of machine learning models toward abnormality detection in chest radiographs,", in *Proc. of 41st Annual Int. Conf. of the IEEE Engineering in Medicine and Biology Society (EMBC)*, 2019, 23-27 July 2019, Berlin, Germany [Online]. Available: IEEE Xplore, https://doi.org/10.1109/EMBC.2019.8856715. [Accessed: 8 May 2022].

[7] R. Hooda, A. Mittal, and S. Sofat, "Lung segmentation in chest radiographs using fully convolutional networks," *Turkish Journal of Electrical Engineering and Computer Science.*, vol.27, pp.710– 722, 2019. doi:10.3906/elk-1710-157

[8] P. Y. Simard, D. Steinkraus, and J. C. Platt, "Best Practices for Convolutional Neural Networks Applied to Visual Document Analysis," in *Proc. of 7th Int. Conference on Document Analysis and Recognition (Icdar) 2003. 6 Aug. 2003, Edinburgh, UK* [Online]. Available: IEEE Xplore, https://doi.org/10.1109/ICDAR.2003.1227801. [Accessed: 8 May 2022].

[9] Y. Lecun, L. Bottou, Y. Bengio, and P. Haffner, "Gradient-based learning applied to document recognition," *IEEE*, vol. 86, no. 11, pp. 2278–2324, 1998. doi:10.1109/5.726791

[10] Y. LeCun, Y. Bengio, and G. Hinton, "Deep learning," *Nature*, vol. 521, pp. 436–444, May 2015. doi:10.1038/nature14539

[11] V. Nair and G. E. Hinton, "Rectified Linear Units Improve Restricted Boltzmann Machines," in *Proc. of ICML'10: 27th International Conference on Machine Learning*, June 21-24, 2010, Haifa, Israel [Online]. Available: Toronto University, http:// https://www.cs.toronto.edu/~fritz/absps/reluICML.pdf. [Accessed: 8 May 2022].

[12] D. C. Cireşan, U. Meier, J. Masci, L. M. Gambardella, and J. Schmidhuber, "Flexible, high performance convolutional neural networks for image classification," in *Proc. of IJCAI'11: the 22th international joint conference on Artificial Intelligence*, vol. 2, July 2011, Barcelona Catalonia, Spain, pp. 1237–1242, [Online]. Available: Acm Digital Library, https://doi.org/10.5591/978-1-57735-516-8/IJCAI11-210. [Accessed: 8 May 2022].

[13] G. E. Hinton, N. Srivastava, A. Krizhevsky, I. Sutskever, and R. R. Salakhutdinov, "Improving neural networks by preventing co-adaptation of feature detectors", *arxiv.org*, Jul. 3, 2012. [Online]. Available: https://arxiv.org/abs/1207.0580. [Accessed: May 8, 2022].

[14] M. D. Zeiler and R. Fergus, "Visualizing and Understanding Convolutional Networks," in *Proc. of 13th European Conference of Computer Vision – ECCV 2014*, 2014, Zurich, Switzerland, September 6-12, 2014, D. Fleet, T. Pajdla, B. Schiele, T. Tuytelaars, Eds. Berlin: Springer, vol. 8689, pp. 818–833.

[15] T.Rahman, M. Chowdhury, and A. Khandakar, "COVID19 Radiography Database*", kaggle.com,* Oct. 3, 2019. [Online]. Available: https://www.kaggle.com/tawsifurrahman/covid19-radiography-database. [Accessed: May 8, 2022].

[16] R. Caruana, "Multitask Learning," *Machine Learning*, vol. 28, no. 1, pp. 41–75, 1997. doi:10.1023/A:1007379606734

[17] S. Thrun, "Is Learning The n-th Thing Any Easier Than Learning The First ?," in *Proc. of Advances in Neural Information Processing Systems 8*, *NIPS*, Denver, CO, USA, November 27-30, 1995, D. S. Touretzky, M. C. Mozer and M. E. Hasselmo, Eds. United States:MIT Press, pp. 640–646, 1996.

[18] J. Deng, W. Dong, R. Socher, L. Li, K. Li, and L. Fei-fei, "ImageNet : a Large-Scale Hierarchical Image Database," in *Proc. of 2009 IEEE Conference of Computer Vision Pattern Recognition.*, 20-25 June 2009, Miami, Florida, [Online]. Available: IEEE Xplore, https://doi.org/10.1109/CVPR.2009.5206848. [Accessed: 8 May 2022].

[19] A. Krizhevsky, I. Sutskever, and G. E. Hinton, "ImageNet classification with deep convolutional neural networks," *Communications of ACM*, vol. 60, no. 6, pp. 84–90, May 2017. doi:10.1145/3065386

[20] K. Simonyan and A. Zisserman, "Very Deep Convolutional Networks for Large-Scale Image Recognition," *arxiv.org*, Sep. 4, 2014. [Online]. Available: http://arxiv.org/abs/1409.1556. [Accessed: May 8, 2022].

[21] S. Han, H. Mao, and W. J. Dally, "Deep compression: Compressing deep neural networks with pruning, trained quantization and huffman coding", *arxiv.org*, Oct. 1, 2015. [Online]. Available: https://arxiv.org/abs/1510.00149. [Accessed: May 8, 2022].

[22] A. G. Howard *et al.*, "MobileNets: Efficient convolutional neural networks for mobile vision applications", *arxiv.org*, Apr. 17, 2017. [Online]. Available: https://arxiv.org/abs/1704.04861. [Accessed: May 8, 2022].

[23] J. Redmon and A. Farhadi, "YOLO9000: Better, Faster, Stronger.", *arxiv.org*, Dec. 25, 2016. [Online]. Available: https://arxiv.org/abs/1612.08242. [Accessed: May 8, 2022].

[24] M. Lin, Q. Chen, and S. Yan, "Network In Network", *arxiv.org*, Dec. 16, 2013. [Online]. Available: https://arxiv.org/abs/1312.4400. [Accessed: May 8, 2022].

[25] Y. Li, W. Wang, and D. Yu, "Application of adaptive histogram equalization to x-ray chest images," in *Proc.of the Second International Conference on Optoelectronic Science and Engineering '94*, 15-18 August 1994, Beijing, China, [Online]. Available: SPIE Digital library, https://doi.org/10.1117/12.182056. [Accessed: 8 May 2022].

[26] R. A. Hummel, "Image enhancement by histogram transformation," *Computer Graphics and Image Processing*, vol. 6, no. 2, pp. 184–195, Apr. 1977. doi:10.1016/S0146-664X(77)80011-7

[27] R.A. Hummel, "Histogram modification techniques," *Computer Graphics and Image Processing*, vol. 4, no. 3, pp. 209–224, Sept. 1975. doi:10.1016/0146-664X(75)90009-X

[28] D.J. Ketcham, "Real-time image enhancement techniques.," *Image Processing*, vol. 74, pp. 120–125, 1976. doi:10.1117/12.954708

[29] S.M. Pizer, "Intensity mappings for the display of medical images.," *Functional mapping of organ systems and other computer topics.*, pp. 205–217, 1981. doi:10.1016/0146-664X(81)90006-X

[30] K. Zuiderveld, *Graphics Gems IV:Contrast limited adaptive histogram equalization*," San Diego, CA, United States: Academic Press Professional, pp. 474–485, 1994.

[31] S. M. Pizer, R. E. Johnston, J. P. Ericksen, B. C. Yankaskas, and K. E. Muller, "Contrast-limited adaptive histogram equalization: speed and effectiveness," in *Proc.of the First Conference on Visualization in Biomedical Computing*, 1990, 22-25 May 1990, Atlanta, GA, USA, [Online]. Available: IEEE Xplore, https://doi.org/10.1109/VBC.1990.109340. [Accessed: 8 May 2022].

[32] A. Narin, C. Kaya, and Z. Pamuk, "Automatic detection of coronavirus disease (COVID-19) using X-ray images and deep convolutional neural networks," *Pattern Analysis and Applications.*, vol. 24, no. 3, pp. 1207–1220, 2021. doi:10.1007/s10044-021-00984-y

[33] F. S. Isabella Castiglioni *et al.*, "Artificial Intelligence Applied on Chest X-Ray Can Aid in the Diagnosis of Covid-19 Infection", *medrxiv.org*, Apr. 10, 2020. [Online]. Available: https://doi.org/10.1101/2020.04.08.20040907. [Accessed: May 8, 2022].

[34] A. Haghanifar, M. M. Majdabadi, and S. Ko, "COVID-CXNet: Detecting covid-19 in frontal chest x-ray images using deep learning", *arxiv.org*, Jun. 16, 2020. [Online]. Available: https://arxiv.org/abs/2006.13807. [Accessed: May 8, 2022].

[35] D. Das, K. C. Santosh, and U. Pal, "Truncated inception net: COVID-19 outbreak screening using chest X-rays," *Physical and Engineering Sciences in Medicine*, vol. 43, no. 3, pp. 915–925, Sep. 2020. doi:10.1007/s13246-020-00888-x

[36] P. Saha, M. S. Sadi, and M. M. Islam, "EMCNet: Automated COVID-19 diagnosis from X-ray images using convolutional neural network and ensemble of machine learning classifiers," *Informatics in Medicine Unlocked*, vol. 22, p. 100505, 2021. doi:10.1016/j.imu.2020.100505

** Bu makale 5th International Conference on Engineering Technologies in Konya/TURKEY (ICENTE 2021) isimli konferansta sunulmuş bildirinin genişletilmiş halidir.*